Electronic Supplementary Information for:

Supramolecular networks in molecular complexes of pyridine boronic acids and polycarboxylic acids: Synthesis, structural characterization and fluorescent properties

José J. Campos-Gaxiola,[a] Blanca A. García-Grajeda,[a] Irán F. Hernández-Ahuactzi,[b] Jorge A. Guerrero-Álvarez,[c] Herbert Höpfl,[c] and Adriana Cruz-Enríquez*[a]

[a] Facultad de Ingeniería Mochis, Universidad Autónoma de Sinaloa, Fuente de Poseidón y Prol. A. Flores S/N, C.P. 81223, C.U. Los Mochis, Sinaloa, México. Tel: (52) 668 8127641; Fax: (52) 668 8127641; E-mail: cruzadriana@uas.edu.mx

[b]Centro Universitario de Tonalá, Universidad de Guadalajara, Campus CU Tonalá, Av. Nuevo Periférico No. 555, Ejido San José Tatepozco, C.P. 45425, Tonalá, Jalisco, México.

[c] Centro de Investigaciones Químicas, Instituto de Investigación en Ciencias Básicas y Aplicadas, Universidad Autónoma del Estado de Morelos. Av. Universidad 1001, C.P. 62209, Cuernavaca, México. Tel., Fax: +52 777 3297997. E-mail: hhopfl@uaem.mx.

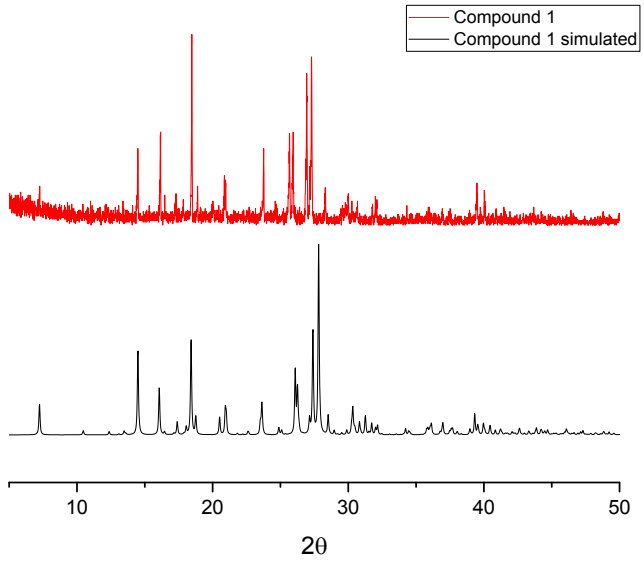

Figure S1. Experimental PXRD pattern for compound **1** in comparison with the pattern simulated from the SXRD analysis. Note: Contrary to the experimental PXRD pattern, which was measured at T = 293 K, the SXRD data were acquired at low temperature (T = 100K), causing a shift of the peaks due to the change of the unit cell parameters.

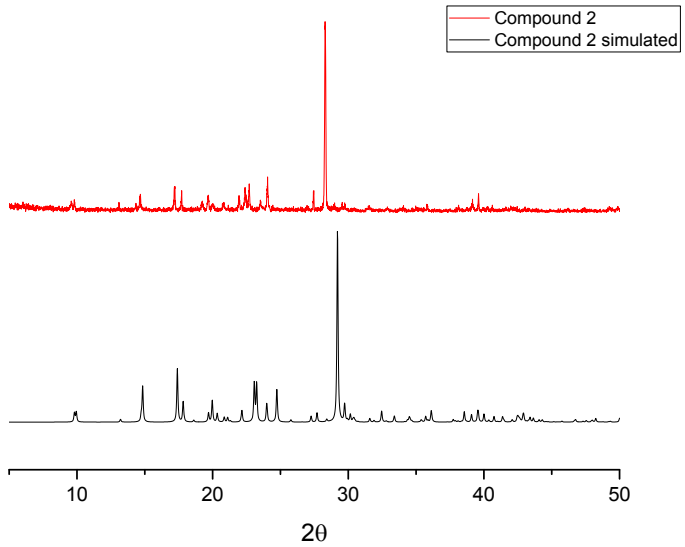

Figure S2. Experimental PXRD pattern for compound **2** in comparison with the pattern simulated from the SXRD analysis. Note: Contrary to the experimental PXRD pattern, which was measured at T = 293 K, the SXRD data were acquired at low temperature (T = 100K), causing a shift of the peaks due to the change of the unit cell parameters.

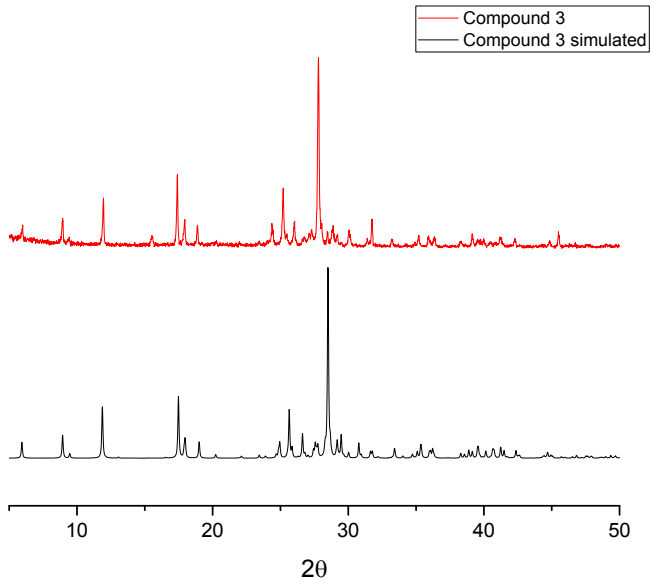

Figure S3. Experimental PXRD pattern for compound **3** in comparison with the pattern simulated from the SXRD analysis. Note: Contrary to the experimental PXRD pattern, which was measured at T = 293 K, the SXRD data were acquired at low temperature (T = 100K), causing a shift of the peaks due to the change of the unit cell parameters.

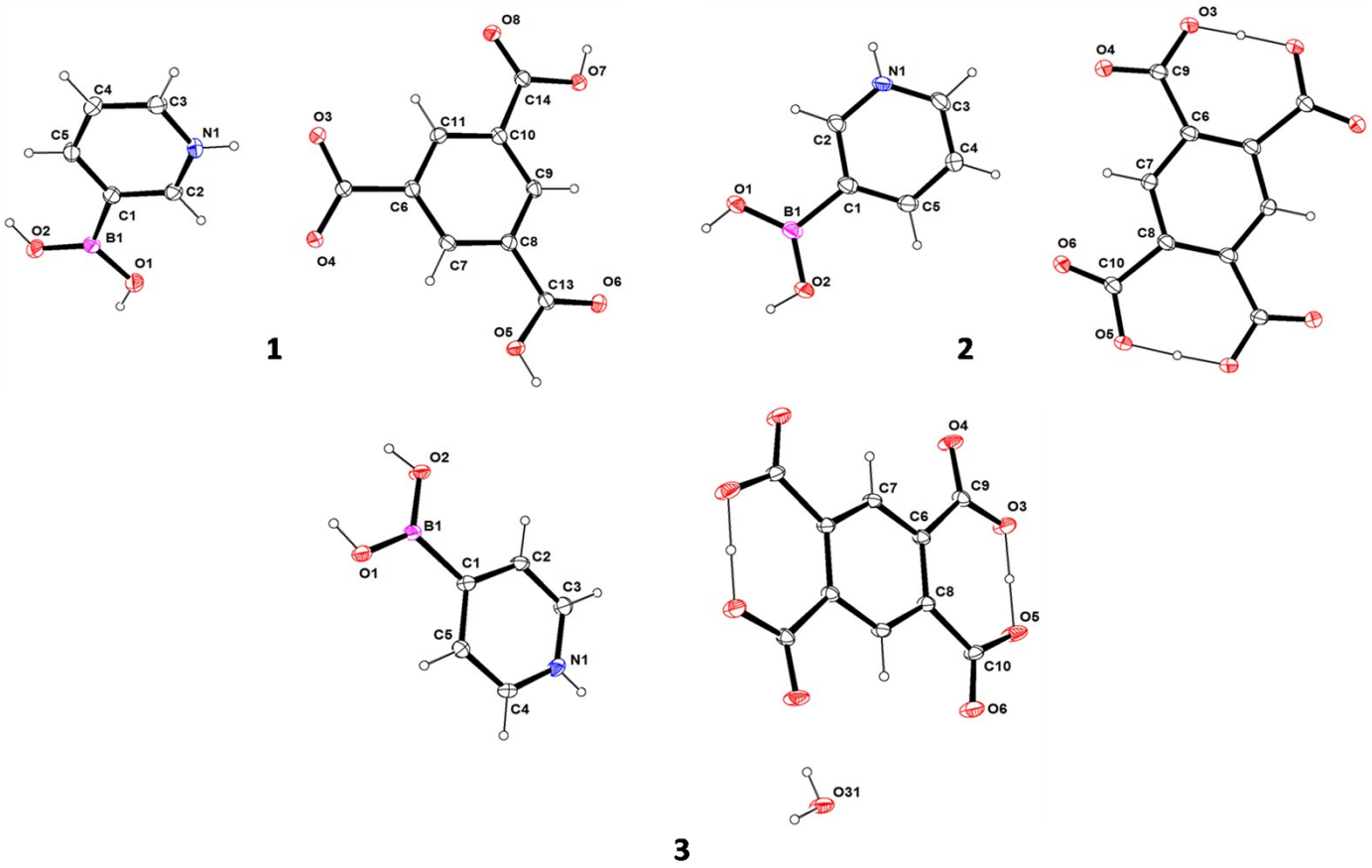

Figure S4. ORTEP diagrams showing the molecular structures of the components in the molecular complexes **1-3** with thermal ellipsoids at the 50% probability level and the atom-labeling scheme.

Table S1. Select bond lengths (Å) and bond angles (°) for the molecular complexes **1-3**.

		1	
B(1)-O(1)	1.3496(19)	O(7)-C(14)	1.3177(17)
B(1)-O(2)	1.3556(19)	O(8)-C(14)	1.2261(17)
B(1)-C(1)	1.589(2)	O(1)-B(1)-O(2)	121.00(13)
N(1)-C(2)	1.3421(19)	O(1)-B(1)-C(1)	116.13(13)
N(1)-C(3)	1.3413(19)	O(2)-B(1)-C(1)	122.86(13)
O(3)-C(12)	1.2660(17)	O(3)-C(12)-O(4)	123.05(12)
O(4)-C(12)	1.2537(17)	O(5)-C(13)-O(6)	124.98(13)
O(5)-C(13)	1.3118(17)	O(7)-C(14)-O(8)	123.99(13)
O(6)-C(13)	1.2183(17)	C(2)-N(1)-C(3)	122.21(13)
		2	
B(1)-O(1)	1.339(2)	O(1)-B(1)-O(2)	126.11(15)
B(1)-O(2)	1.340(2)	O(1)-B(1)-C(1)	115.66(15)
B(1)-C(1)	1.571(2)	O(2)-B(1)-C(1)	118.20(15)
N(1)-C(2)	1.328(2)	O(3)-C(9)-O(4)	121.23(15)
N(1)-C(3)	1.326(2)	O(5)-C(10)-O(6)	122.60(14)
O(3)-C(9)	1.278(2)	C(2)-N(1)-C(3)	121.98(14)
O(4)-C(9)	1.215(2)		
O(5)-C(10)	1.279(2)		
O(6)-C(10)	1.2154(19)		
		3	
B(1)-O(1)	1.355(3)	O(1)-B(1)-O(2)	126.2(1)
B(1)-O(2)	1.350(3)	O(1)-B(1)-C(1)	117.4(2)
B(1)-C(1)	1.595(3)	O(2)-B(1)-C(1)	116.4(2)
N(1)-C(3)	1.341(3)	O(3)-C(9)-O(4)	120.7(2)
N(1)-C(4)	1.342(3)	O(5)-C(10)-O(6)	121.8(2)
O(3)-C(9)	1.293(3)	C(3)-N(1)-C(4)	122.3(2)
O(4)-C(9)	1.219(3)		
O(5)-C(10)	1.286(3)		
O(6)-C(10)	1.230(3)		

Table S2. Geometrical parameters (Å/°) for the moieties involved in π-π stacking interactions and B-π contacts in the crystal structures of the molecular complexes **1-3**.

Compound	Cg(I)···Cg(J)	B-π (B···C)	α	β	γ	π-stacking styles
1	3.66	_	0.00	22.21	22.21	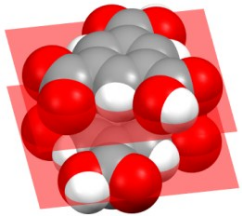
	4.95	3.44	0.00	54.74	54.74	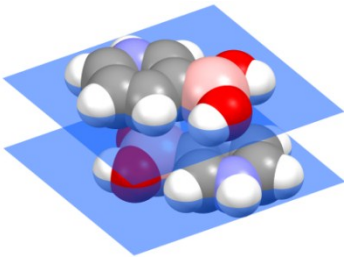
	5.49	3.62	0.00	47.81	47.81	
2	3.23	_	5.46	21.78	21.39	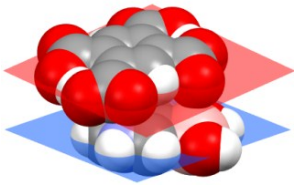
3	3.66	_	0.00	22.90	22.90	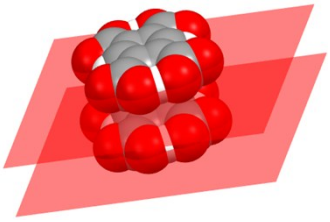
	3.66	3.56 and 3,57	0.00	22.04	22.04	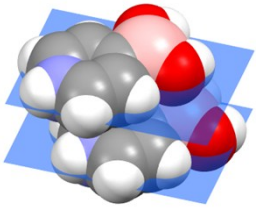

Cg···Cg: centroid-centroid distance; α: dihedral angle between the ring planes; β: angle between the centroid vector Cg(I)···Cg(J) and the normal to the plane I; γ: angle between the centroid vector Cg(I)···Cg(J) and the normal to the plane J.

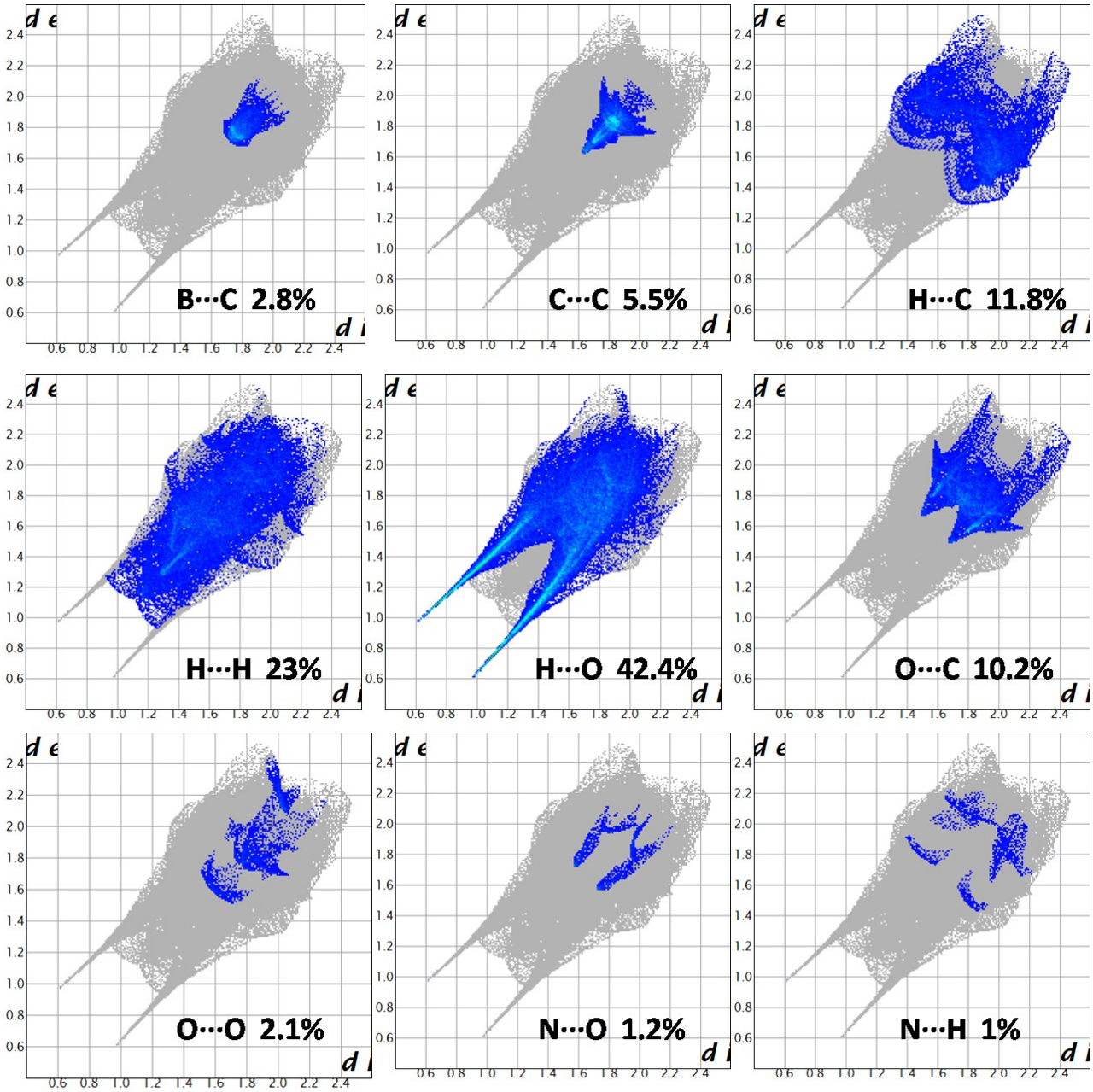

Fig. S5. Decomposed two-dimensional fingerprint plots for compound **1**. Close contacts and their relative contributions are indicated.

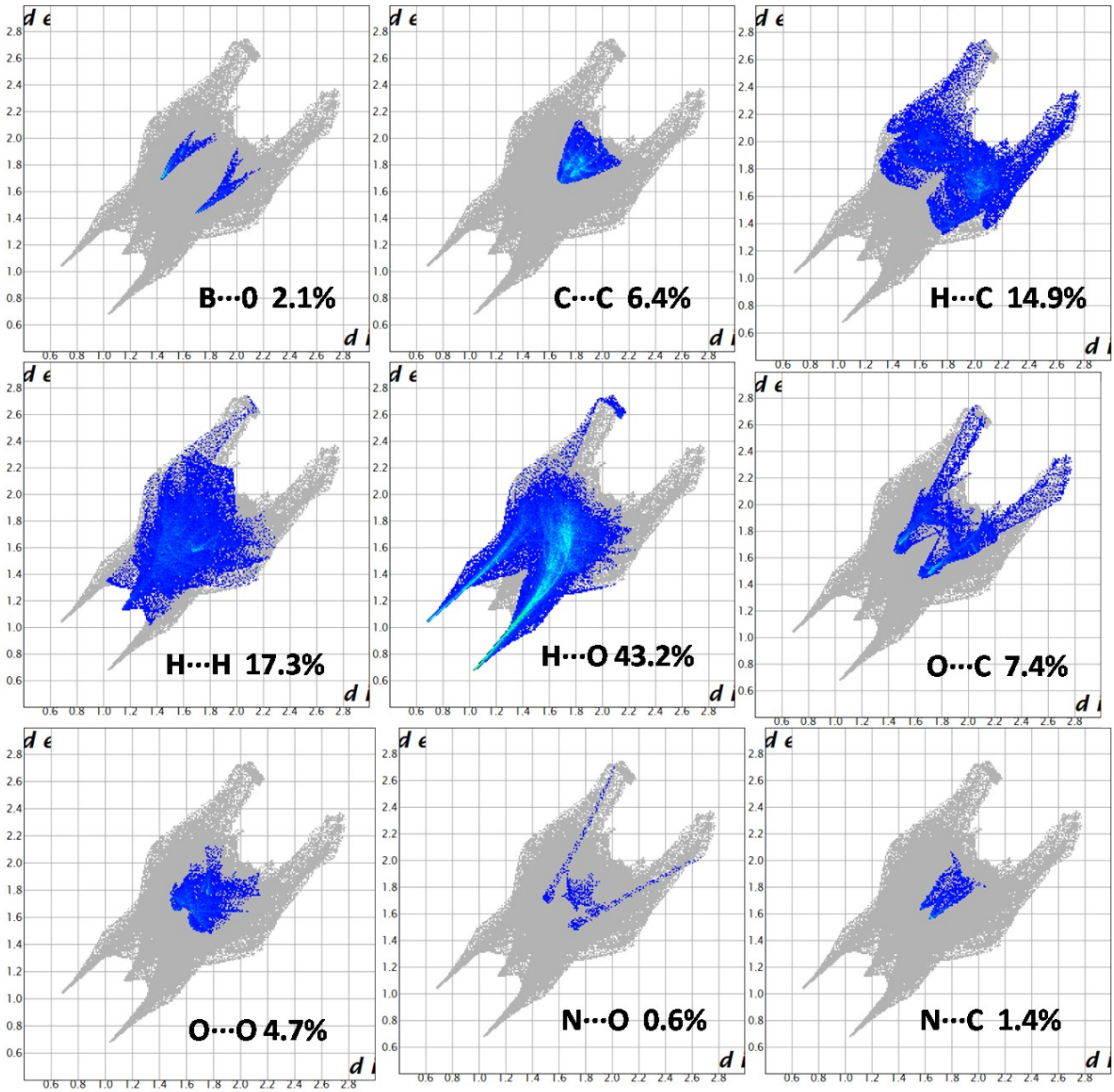

Fig. S6. Decomposed two-dimensional fingerprint plots for compound **2**. Close contacts and their relative contributions are indicated.

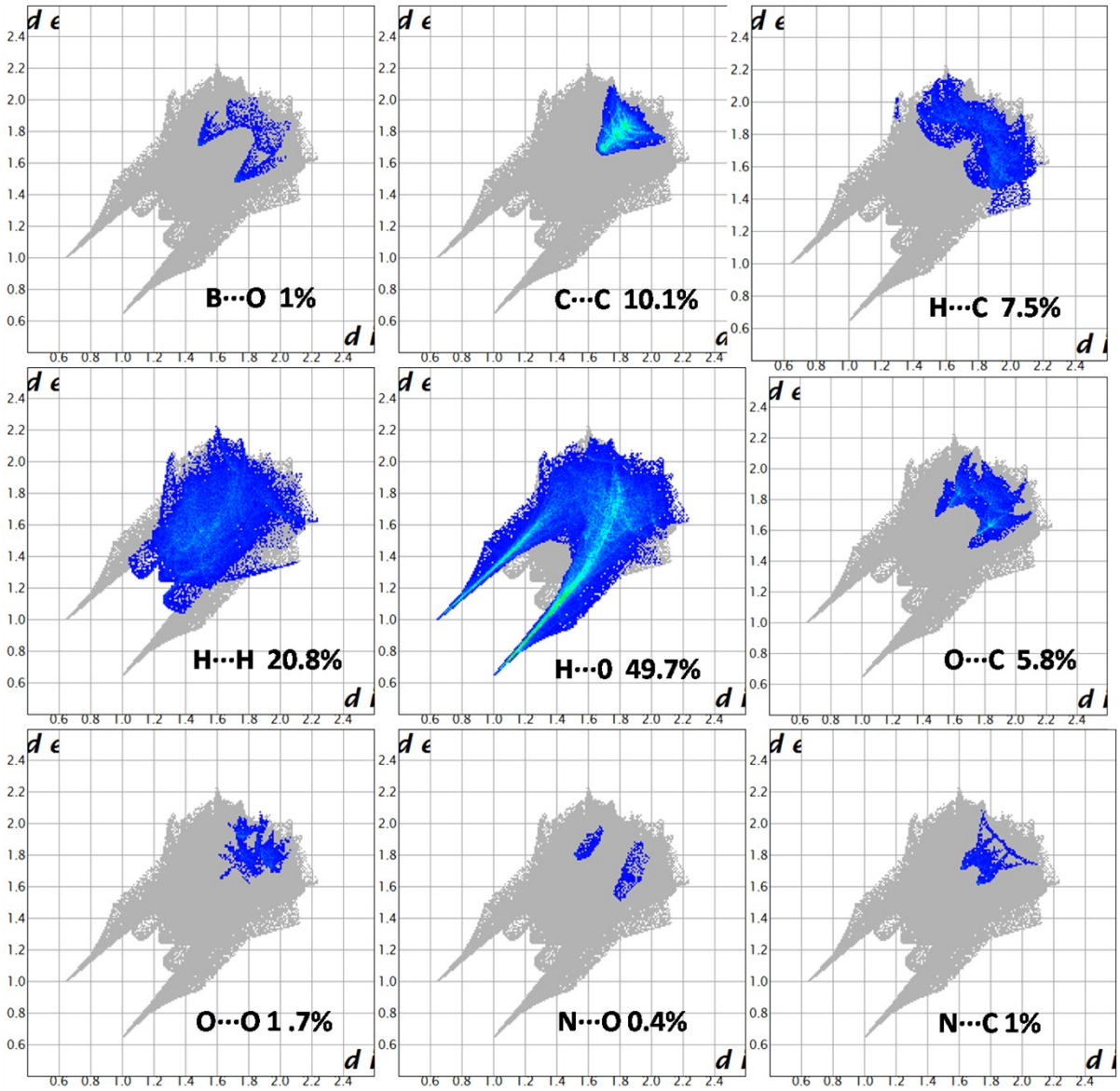

Fig. S7. Decomposed two-dimensional fingerprint plots for compound **3**. Close contacts and their relative contributions are indicated.

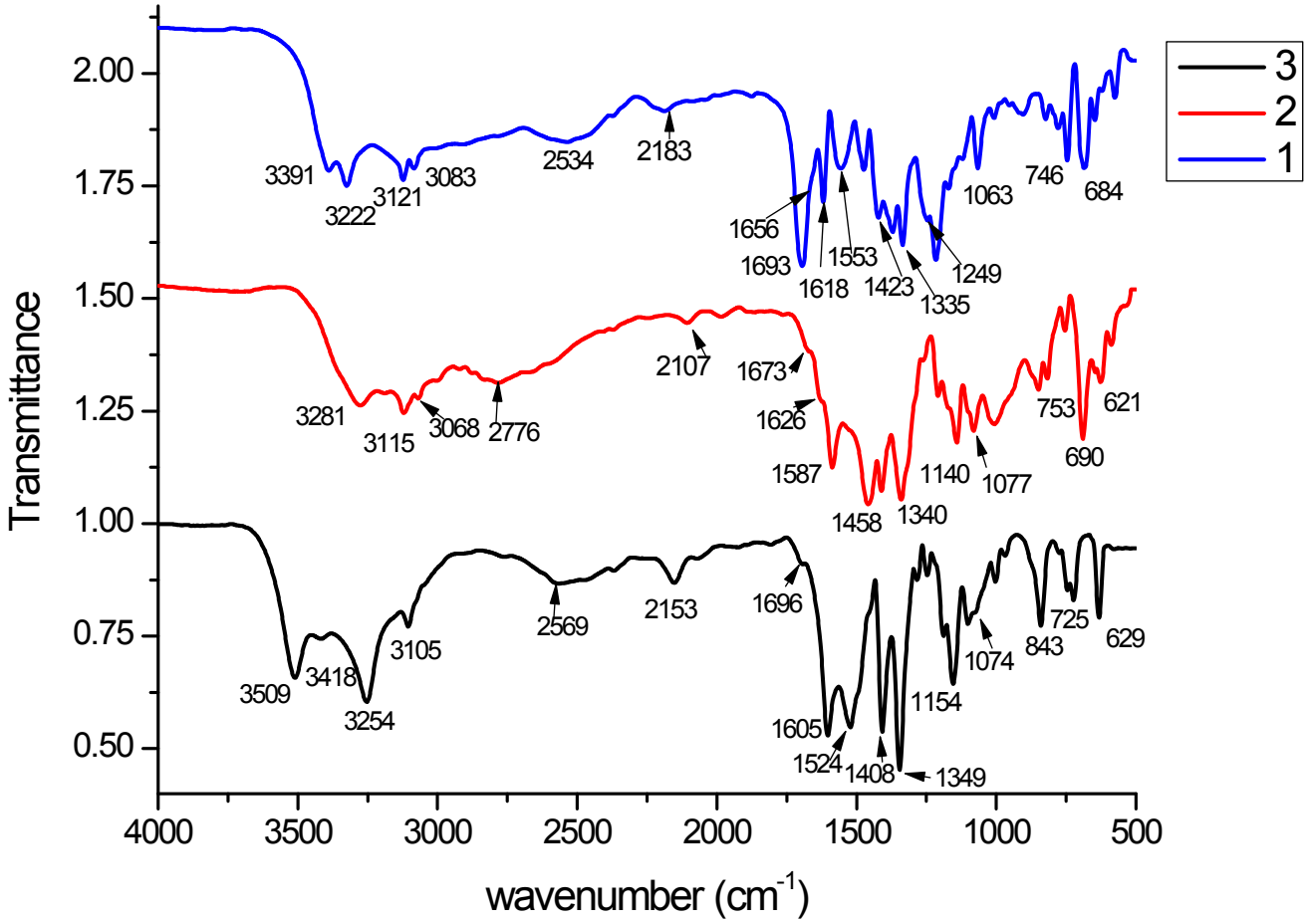

Fig. S8. IR spectra of compounds **1-3**.

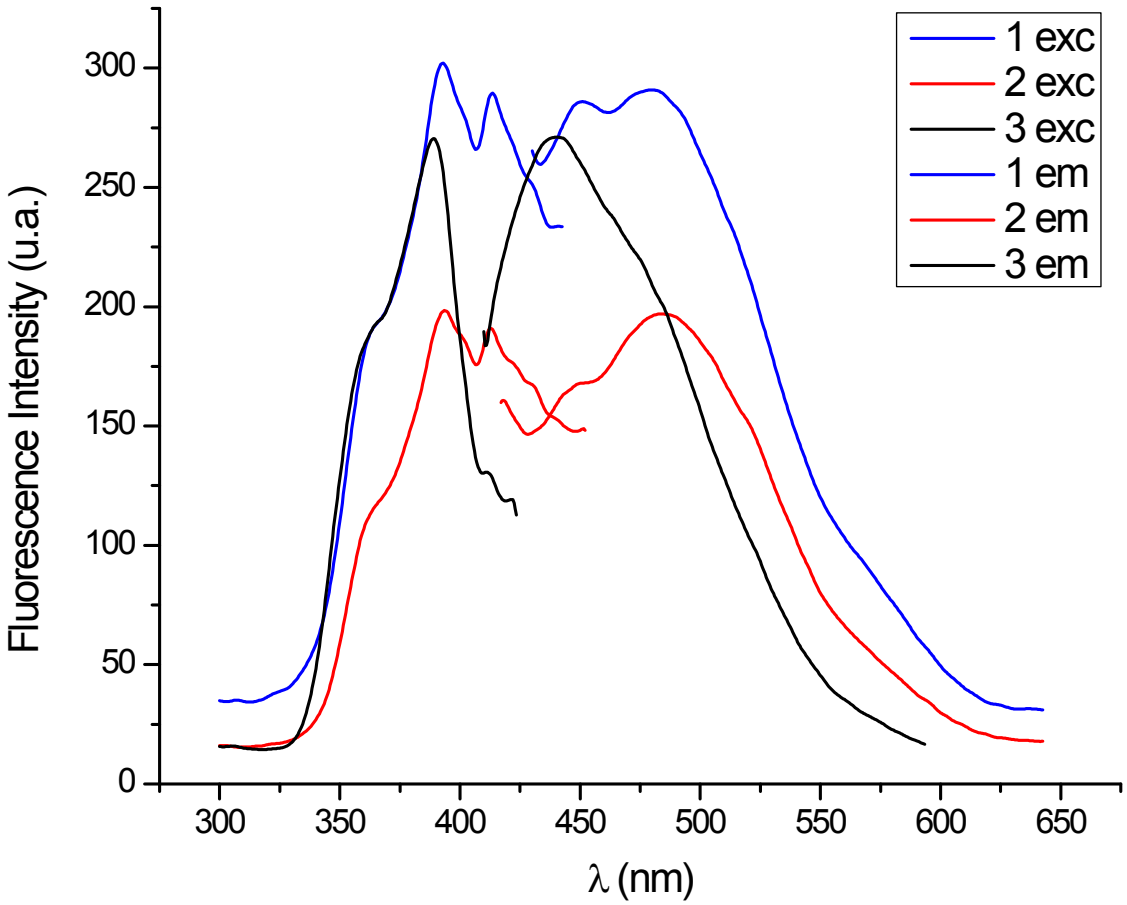

Fig. S9. Solid-state excitation and emission spectra for **1**, **2** and **3** at room temperature.

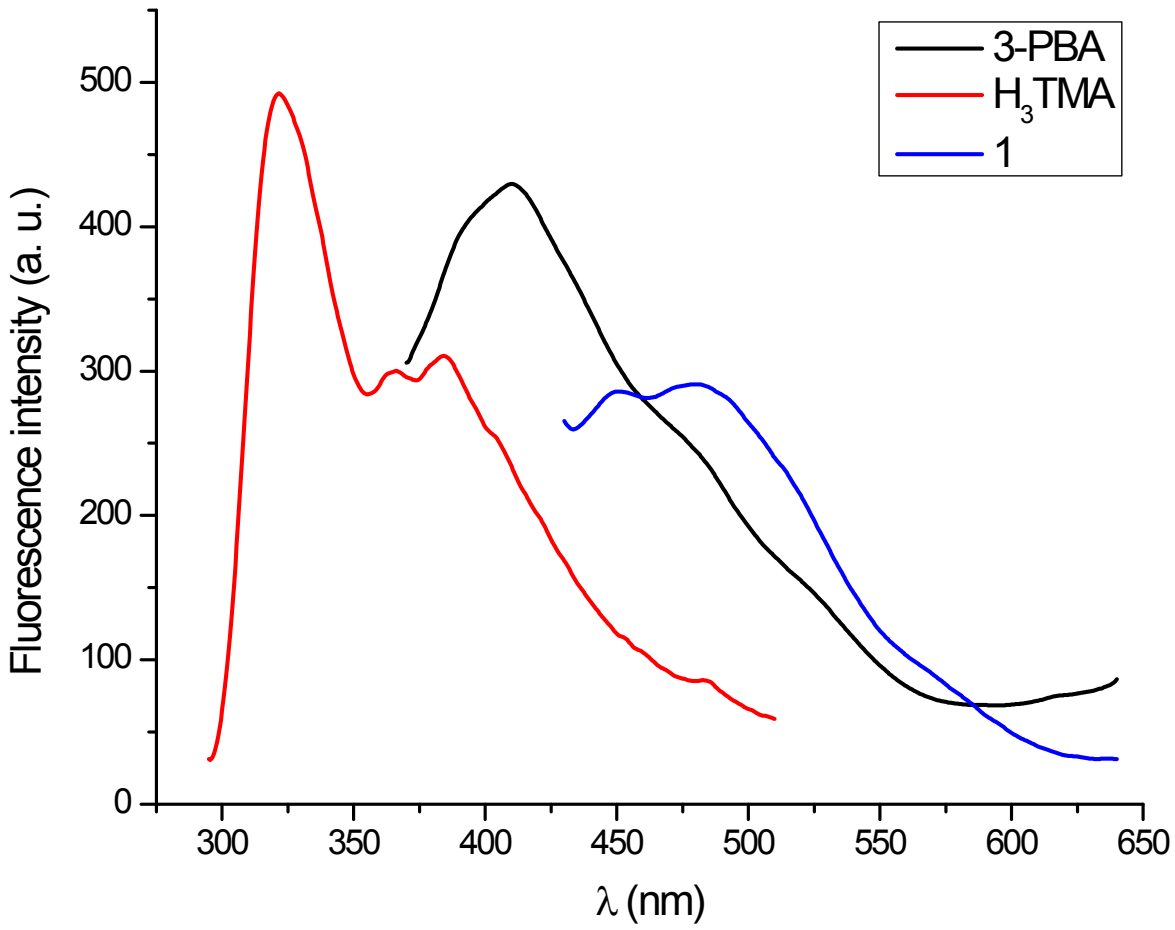

Fig. S10. Solid-state emission spectra of 3PBA, H_3TMA and **1** at room temperature.

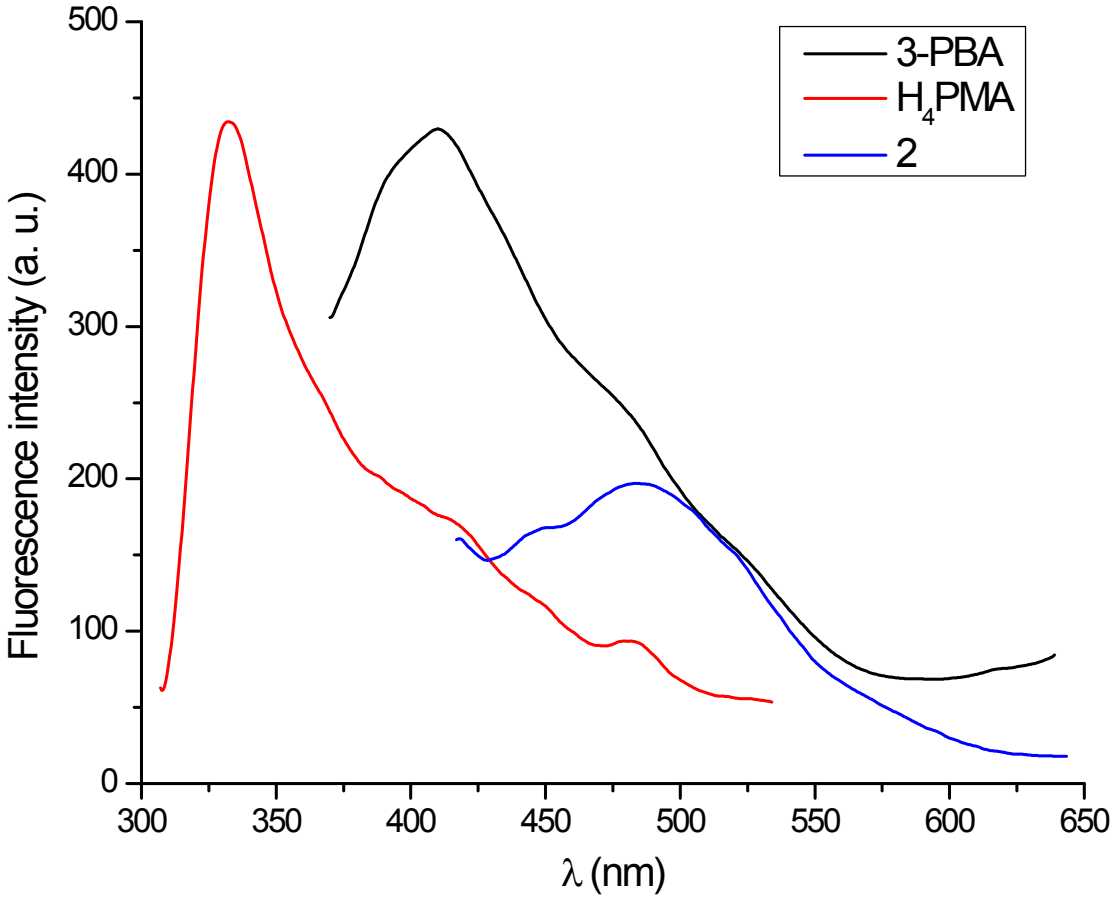

Fig. S11. Solid-state emission spectra of 3PBA, H_4PMA and **2** at room temperature.

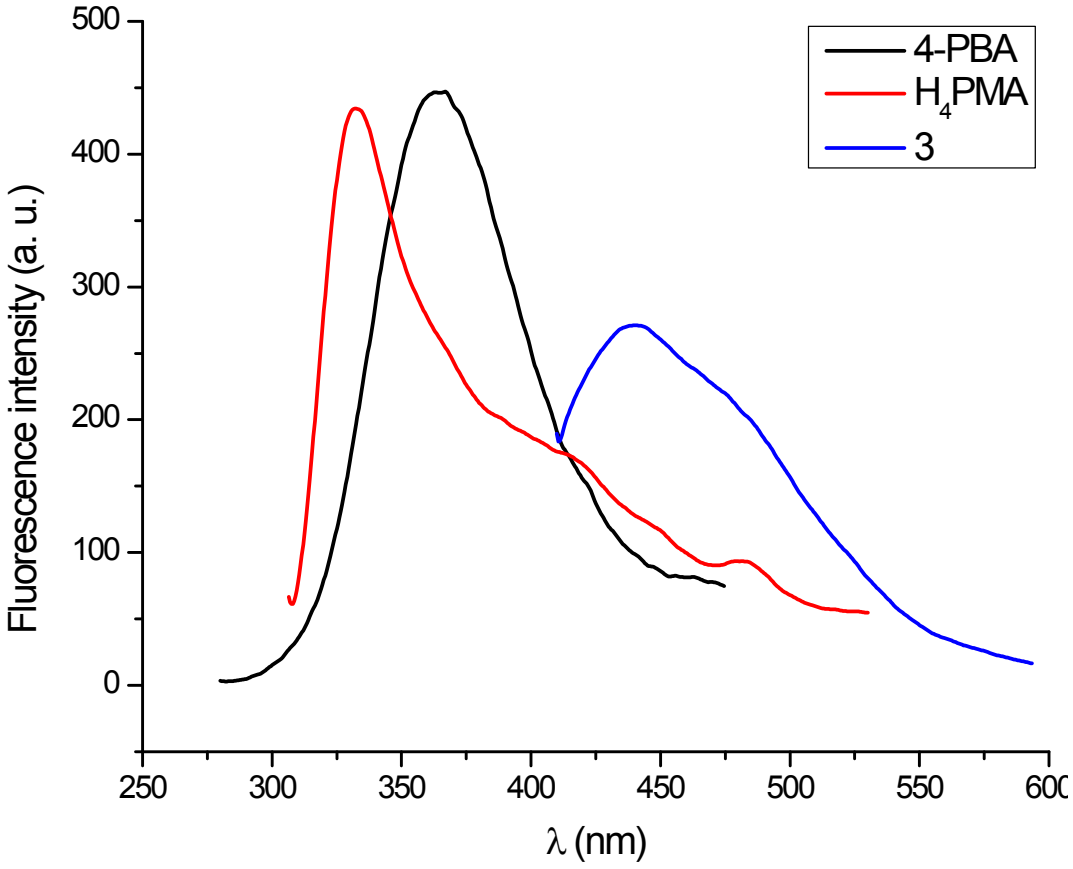

Fig. S12. Solid-state emission spectra of 4PBA**,** H_4PMA and **3** at room temperature.